



Universiteit
Leiden
The Netherlands

Influence of the electrode-electrolyte interface on electrochemical CO₂ reduction reaction and hydrogen evolution reaction

Ye, C.

Citation

Ye, C. (2024, December 5). *Influence of the electrode-electrolyte interface on electrochemical CO₂ reduction reaction and hydrogen evolution reaction*. Retrieved from <https://hdl.handle.net/1887/4170871>

Version: Publisher's Version

License: [Licence agreement concerning inclusion of doctoral thesis in the Institutional Repository of the University of Leiden](#)

Downloaded from: <https://hdl.handle.net/1887/4170871>

Note: To cite this publication please use the final published version (if applicable).

Chapter 4

The Role of Cations in Hydrogen Evolution Reaction on a Platinum Electrode in Mildly Acidic Media

This chapter is based on:

Ye, C.; Liu, X.; Koper, M. T. M. *Eletrochem. Commun.* **2024**, 166, 107784

Abstract: In this work, we study the influence of cation concentration and identity on the hydrogen evolution reaction (HER) on polycrystalline platinum (Pt) electrode in pH 3 electrolytes. Our observations indicate that cations in the electrolyte do not affect proton reduction at low potentials. However, an increase in cation concentration significantly enhances water reduction. Simultaneously, we identify a non-negligible migration current under mass transport limited conditions in electrolytes with low cation concentration. To separate migration effects from specific cation-promotion effects on HER, we carried out further experiments with electrolytes with mixtures of Li^+ and K^+ cations. Our results show that, adding strongly hydrated cations (Li^+) to a K^+ -containing electrolyte leads to a less negative onset potential of water reduction. Interfacial pH measurements reveal a same interfacial pH at the platinum electrode in pH 3 in the presence of 80 mM LiClO_4 and KClO_4 , respectively, at potentials where water reduction occurs. Based on these results, we suggest that under the current conditions, the strongly hydrated cations (Li^+) promote water dissociation on the Pt electrode more favorably in comparison with the more weakly hydrated cations (K^+).

4.1 Introduction

Catalyzing water splitting, specifically water reduction to produce hydrogen, stands at the forefront of electrochemical research due to its fundamental significance and profound implications for a sustainable energy future. Extensive work has been dedicated to develop efficient catalysts and to gain mechanistic insights of the hydrogen evolution reaction process.¹⁻¹³ Traditionally, the significant variations in HER rates (up to few orders of magnitude) observed on different electrode materials have been correlated to differences in the free energy of hydrogen adsorption.¹⁴⁻¹⁵ However, this adsorption energy-based descriptor has certain limitations, notably in its inability to describe the sluggish kinetics of HER in alkaline media,^{9, 16} where water dissociation is a prerequisite for generating adsorbed hydrogen. Further, it is crucial to note that the electrochemical environment at the metal-electrolyte interface profoundly influences HER activity under alkaline conditions. Consequently, other descriptors, which extend beyond mere adsorption energies, have gained attention. These include interfacial descriptors, such as the interfacial field strength, the oxophilicity of the surface sites and the cation solvation energy, all of which contribute to a more comprehensive understanding of the HER mechanism.^{2, 5, 8, 17-18} In particular, these descriptors capture the delicate balance between the charge transfer-induced water dissociation step ($H_2O + e^- + * \rightarrow H-* + OH^-$), the favorable/unfavorable interactions of the dissociation products with the surface (H_{ad} and OH_{ad}) and/or concomitant rates of the H_{ad} recombination step (H_2 production) and desorption of OH_{ad} , thereby influencing HER kinetics in alkaline media.

Metal cations in the electrolyte have been shown to have a significant effect on HER activity in alkaline media. Strmcnik et al have shown that HER kinetics on transition metal hydroxide modified Pt electrodes improves in Li^+ containing electrolytes, which they attribute to the stabilizing effect of Li^+ ions on the adsorbed hydroxyl ($*OH-cat^+$) species at the interface.¹⁹⁻²⁰ Using a similar system, Liu et al suggest that the driving force for OH desorption is larger for Li^+ than for Na^+ and K^+ , thereby giving rise to the HER activity decreasing in the order $LiOH > NaOH > KOH$ at pH 13.²¹ These studies attributed the promotion of the

electrochemical water dissociation step to favorable cation-water interactions. However, these descriptors fail to elucidate the inverted activity trend ($K^+ > Na^+ > Li^+$) observed on a gold electrode in 0.1 M XOH.²² Also, increasing Na^+ cation concentration significantly enhances HER activity on a gold electrode up to pH 11 while the opposite trends have been observed at a higher pH (pH > 12).⁹ In the latter work, the enhanced HER activity was linked to favorable interaction of the cation with the dissociating water molecule ($*H-OH^{\delta-}-cat^+$), resulting from the increased near-surface cation concentration due to the local field strength.^{9, 12} The decreased HER activity at high pH was attributed to a blockage or crowding effect caused by cation accumulation at the interface.^{9, 12} These findings underscore the convoluted role of different interfacial parameters in tuning the activity of HER on a given surface in alkaline media.

Understanding the activity trend for the HER is also crucial for the development of other renewable energy technologies, such as electrochemical carbon dioxide reduction (CO_2RR), where HER acts as a competing side reaction.^{13, 23-25} Conventionally, CO_2RR electrolyzers have utilized neutral and alkaline electrolyte. However, recent studies highlight the potential of achieving high selectivity for CO_2RR products in acidic media.²⁶⁻³⁰ Although the fast kinetics of the proton reduction remains a concern for CO_2RR in acidic media, it is noteworthy that the interfacial pH near the catalyst depends on specific reaction conditions. Liu et al. have shown a potentially high alkaline interfacial pH at a Au disk electrode during CO_2RR in pH 3 electrolytes.³¹ The increased interfacial pH at electrodes with negative-going applied potential suggests water reduction over a broad potential window as the competitive reaction with CO_2RR .

When probing the effect of cation concentration on HER kinetics, one needs to consider the effect that cations may have on the migration current. Therefore, in this study, we have systematically investigated the influence of cation concentration and identity on the HER activity on a polycrystalline Pt electrode in pH 3 electrolytes using a background electrolyte mixture of two alkali cations, Li^+ and K^+ . In particular, we show that cations in the electrolyte do not influence proton reduction kinetically. However, with the increasing metal cation

concentration, the water reduction current significantly improves while the diffusion limited current due to proton reduction decreases. This proton migration current is effectively suppressed with excess supporting electrolyte. From the mixed cation electrolyte, we show a promotion effect of strongly hydrated cations (Li^+) on the onset potential of water reduction. We also measure interfacial pH at the polycrystalline electrode during linear sweep voltammetry, revealing pH changes correlating with current density and reaction process. Overall, our study thereby provides valuable insights into the intricate interplay of cation effects on HER in mild acidic media.

4.2 Experimental Section

Chemicals and cell preparation. In this work, all electrolytes were prepared from HClO_4 (Sigma-Aldrich, Ultrapure, 70%), LiClO_4 (Sigma-Aldrich, $\geq 99.99\%$ trace metal basis), KClO_4 (Sigma-Aldrich, $\geq 99.99\%$ trace metal basis), H_2SO_4 (Merck, Suprapur, 96%) and ultrapure water (resistivity $> 18.2 \text{ M}\Omega\cdot\text{cm}$, Millipore Milli-Q). Prior to each experiment, all cell compartments were cleaned by storing them in an acidic potassium permanganate solution ($1 \text{ g}\cdot\text{L}^{-1} \text{ KMnO}_4$ (Fluka, ACS reagent) in $0.5 \text{ M H}_2\text{SO}_4$ (Fluka, ACS reagent)) overnight. The solution was subsequently drained and the cell compartments were rinsed with a dilute piranha solution (1:3 v/v of H_2O_2 (Merck, Emprove exp) / H_2SO_4) to remove residual KMnO_4 and MnOx . Afterwards, the cell compartments were cleaned by repetitive rinsing and boiling with Milli-Q water to remove all inorganic contaminants.

Preparation of polycrystalline platinum (Pt) disk electrode. A polycrystalline platinum (Pt) disk electrode in E6/E5 ChangeDisk tips embedded with a PEEK shroud (Pine Research) was used as working electrode. Prior to the electrochemical experiments, the polycrystalline Pt disk electrode was mechanically polished on a microcloth (Buehler) for 2 min with 1, 0.25 and $0.05 \mu\text{m}$ diamond suspension (MetaDi, Buehler), respectively. After mechanical polishing, the obtained working electrode was sonicated in Milli-Q water for 15 min and rinsed with Milli-Q water. The obtained polycrystalline Pt disk electrode was then mounted on the rotating disk electrode (RDE) tip for electrochemical experiments.

Electrochemical measurements. All electrochemical experiments were carried out with a BioLogic potentiostat (SP-300) and a modulated speed rotator (Pine Research) in a standard three-electrode electrochemical cell. A Pt wire (0.5 mm diameter, MaTecK, 99.9%) was used as the counter electrode, a leakless Ag/AgCl (EDAQ) was used as the reference electrode. All reported potentials were converted to the reversible hydrogen electrode scale. Prior to each experiment, argon (Linde, 6.0) was purged through the electrolyte for at least 20 min. Next, the polycrystalline Pt disk electrode was electrochemically polished in 0.1 M H₂SO₄ between 0.06 and 1.65 V vs RHE for 200 cycles at 0.5 V s⁻¹. Thereafter, blank cyclic voltammograms were then taken at a scan rate of 50 mV s⁻¹ in the same potential window to characterize the surface, as shown in Figure C.1. For calculating the current densities for the HER activity, the electrochemical active surface area (ECSA) was determined from the integral of the hydrogen region (0.06 to 0.6 V, 230 $\mu\text{C cm}^{-2}$).³² The obtained working electrode was then used for subsequent hydrogen evolution experiments. The experiment in the absence of metal cations was performed in 1 mM HClO₄ (pH 3). In case of different cation concentration electrolytes, the calculated amounts of salt (LiClO₄ or KClO₄) were added to the prepared solution of 1 mM HClO₄. For all hydrogen evolution experiments, the solution resistance was determined by carrying out electrochemical impedance spectroscopy (EIS). The electrode potential was compensated for 100% of ohmic drop for the electrolytes with cation concentration less than 10 mM and 85% of the ohmic drop for all other electrolytes.

RRDE pH measurements. A ring-disk electrode (Au ring and Pt disk, E6/E5 ChangeDisk, Pine Research), a Pt wire (0.5 mm diameter, MaTecK, 99.9%) and a Ag/AgCl electrode were used as working electrode, counter electrode and reference electrode respectively. The Au ring and Pt disk electrodes were mechanically polished separately in the same manner as the Pt rotating disk electrode and then assembled. Afterward, the Pt disk was electrochemically polished and characterized in the same manner with Pt rotating disk electrode. In the meantime, the Au ring was prepared according to previous reported work.^{31, 33} Specifically, the Au ring was characterized in argon-saturated 0.1 M H₂SO₄ by cyclic voltammetry at 100 mV s⁻¹ between 0 to 1.75 V vs RHE. Next, the Pt disk was changed into a Teflon counterpart and the RRDE tip was dipped into a 1 mM 4-nitrothiophenol (4-NTP, Merck, 80%) dissolved

in ethanol (96%, absolute, VWR) solution for 20 min, during which the nitro compound self-assembles as a monolayer on the Au ring. The obtained modified Au ring was then rinsed with ethanol and water respectively, and dried in a N₂ flow. The Pt disk was reassembled carefully and the 4-NTP on the Au ring was further converted to the pH sensing redox couple 4-nitrosothiophenol (4-NSTP)/hydroxylaminothiophenol (4-HATP) via cyclic voltammetry in 0.1 M H₂SO₄ from 0.68 to 0.11 vs RHE at 100 mV s⁻¹. A lower vertex potential of 0.11 V vs RHE was set to maximize the conversion efficiency.

The cyclic voltammograms of the 4-NSTP/4-HATP pH sensing couple were continuously recorded at a scan rate of 200 mV s⁻¹ while the linear sweep voltammetry was performed on Pt disk. The potential window for cyclic voltammetry on the 4-NSTP/4-HATP pH sensing couple modified Au ring was adjusted positively with the increase of the interfacial pH. Details of the calculations of the interfacial pH are identical as listed in the Electronic Supplementary Material of a previously reported work from our group.³¹

4.3 Results and Discussion

4.3.1 Results

First, we examine the cation concentration effect on HER activity on a polycrystalline Pt electrode. Figure 4.1 shows HER current on a Pt polycrystalline electrode at 2400 rpm in pH 3 electrolytes in the presence of 5, 10, 50, 80 and 130 mM LiClO₄ respectively, and the corresponding Tafel slope derived therefrom (see also Figure C.2 in the Supporting Information). Due to the low hydronium ion (H₃O⁺) concentration in pH 3 electrolytes, the proton donor for HER shifts from hydronium ions (H₃O⁺) at low overpotentials to water (H₂O) at high overpotentials, which is reflected in the linear sweep voltammograms in Figure 4.1. As shown in Figures 4.1a, b, the proton reduction current and Tafel slopes of ca. 39 mV/dec are the same in all electrolytes at low overpotentials, which implies the same mechanism and shows that the cation concentration does not affect the proton reduction in kinetically limited regime. At intermediate potentials (~-0.2 - -0.7 V), there is a mass transport limited plateau, which is due to the limited mass transfer of hydronium ions (H₃O⁺) to the surface of the

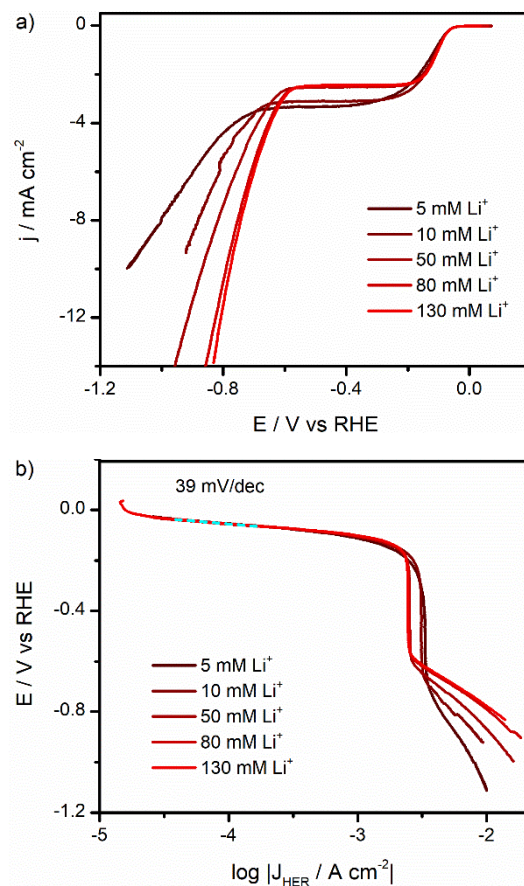


Figure 4.1 Cation (Li^+) concentration effect on HER. a) Linear sweep voltammograms obtained on a polycrystalline Pt electrode at 2400 rpm in pH 3 HClO_4 electrolyte in the presence of 5, 10, 50, 80 and 130 mM LiClO_4 respectively. Scan rate: 10 mV s^{-1} . b) Tafel slope analysis derived from the linear sweep voltammograms shown in a), the range used for fitting is indicated in all plots with a dotted line in blue. A Tafel slope plot of Figure 4.1a is given in the Supporting Information, Figure C.2.³⁴

electrode. At further negative potentials, the water reduction reaction sets in. Notably, with the increase of Li^+ cation concentration, the water reduction current is enhanced significantly with the increasing Li^+ cation concentration in these electrolytes. As shown in Figure C.2b, the obtained Tafel slopes for water reduction are high ($> 120 \text{ mV/dec}$), but become lower with increasing concentration of Li^+ (from ca 800 to ca.300 mV/dec), suggesting strong non-potential dependent contributions to the current. On the other hand, the diffusion limited current decreases with increasing Li^+ cation concentration in the electrolyte. The same trend

has also been observed in pH 3 electrolytes with the presence of 1, 2, 5, 10, 50 and 80 mM KClO_4 , as shown in Figure C.3. Additionally, no clear diffusion limited plateau was observed in pH 3 electrolytes in the presence of 1 and 2 mM KClO_4 . This result suggests that the mass transport limited current is strongly distorted in electrolytes with low cation concentrations. Despite the fact that other factors, such as cation hydrolysis and cation-modified diffusion coefficient of protons,³⁵⁻³⁶ may contribute to the decreased mass transport limited current, our result suggests the non-negligible H_3O^+ migration current in pH 3 electrolytes with a low cation concentration.³⁷ This migration component adds further complexity in understanding the cation effect on HER in pH 3 electrolytes.

However, the migration current near the electrode can be greatly suppressed by introducing a excess supporting electrolyte.³⁸ Figure 4.1 shows a (relatively) stable mass transport limited current in the presence of at least 50 mM LiClO_4 . Therefore, to minimize the migration current, we select 80 mM perchlorate as the supporting electrolyte, in which the diffusion limited current is identical to that calculated by the Levich equation (2.59 mA cm^{-2} under our working conditions).

Figure 4.2 shows the HER activity on a polycrystalline Pt electrode in pH 3 electrolytes with 80 mM KClO_4 or LiClO_4 as the supporting electrolyte. While the proton reduction current remains constant at low overpotentials in all electrolytes, the water reduction is notably influenced by the cations present in the electrolytes. Specifically, an onset potential of ca. -0.70 V vs RHE for water reduction is observed in pH 3 electrolyte in the presence of 80 mM K^+ . Under the same conditions, the onset potential for water reduction in pH 3 electrolyte with 80 mM Li^+ is approximately -0.57 V vs RHE. Moreover, the onset potential of water reduction shifts positively with increasing Li^+ concentration in pH 3 electrolyte with 80 mM K^+ as the supporting electrolyte. On the other hand, the water reduction current (both onset potential and activity) remains constant despite the increased K^+ concentrations in pH 3 electrolyte with 80 mM Li^+ as the supporting electrolyte (Figure 4.2b).

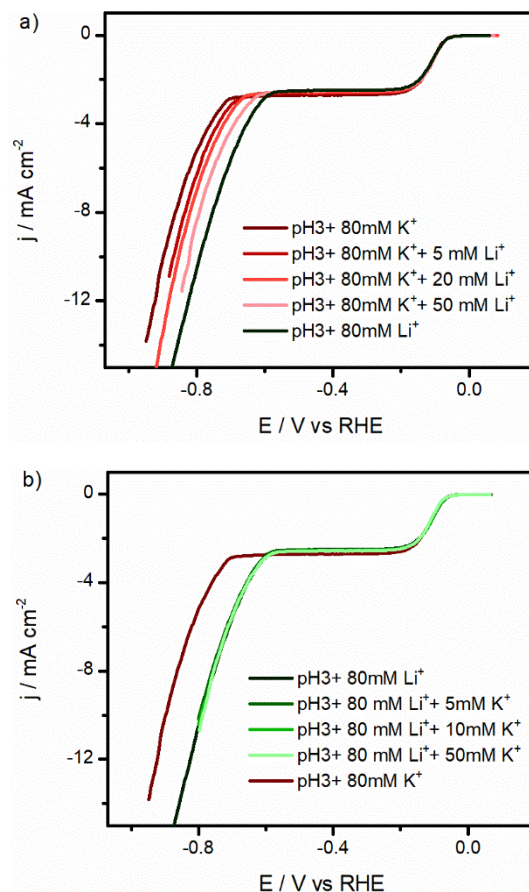


Figure 4.2 Linear sweep voltammograms obtained for the HER on a polycrystalline Pt electrode at 2400 rpm in pH 3 electrolytes. a) In the presence of 80 mM KClO_4 + x mM LiClO_4 and 80 mM LiClO_4 . b) In the presence of 80 mM LiClO_4 + x mM KClO_4 and 80 mM KClO_4 , where x represents 0, 5, 10, 20 or 50 respectively. Scan rate: 10 mV s^{-1} . A cation concentration reaction order plot for the HER current in Fig.4.2a is shown in Figure C.4 in the Supporting Information.

Tafel slopes for water reduction derived from linear sweep voltammograms in Figure 4.2 are given in Figure C.5. The obtained Tafel slopes for water reduction remains constant in all electrolytes, which suggest the same (or similar) kinetics of water reduction in all electrolytes. Simultaneously, the obtained cation concentration reaction order plot shown in Figure C.4 indicates the promoting effect of Li^+ in water reduction. This promotional effect of strongly hydrated cations (Li^+) on the activity of water reduction on polycrystalline Pt has been observed previously; we note the inhibition effect of K^+ on water reduction reported in that work was observed under strongly (bulk) alkaline conditions.^{10, 12, 19}

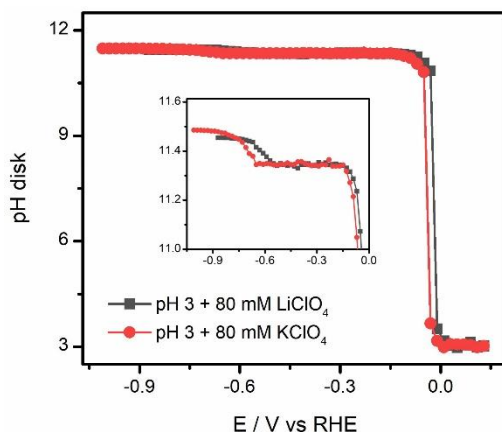


Figure 4.3 The interfacial pH at the Pt disk electrode as a function of potential during linear sweep voltammetry at 2400 rpm and 10 mV s^{-1} in pH 3 electrolytes in the presence of 80 mM LiClO_4 and KClO_4 respectively, as measured using RRDE voltammetry.

To gain additional insights into the mechanism underlying the observed cation effect, the interfacial pH of the Pt disk electrode during LSV is measured with RRDE using a voltammetric pH sensor on the ring.^{31, 33} Figure 4.3 shows the measured interfacial pH at the Pt disk electrode during linear sweep voltammetry in pH 3 electrolytes in the presence of 80 mM LiClO_4 and KClO_4 respectively. The increase in current density during the negative going sweep leads to a continuous consumption of H_3O^+ or an increasing generation of OH^- near the surface of the Pt disk electrode. As a result, the interfacial pH rises simultaneously with the current density. As shown in Figure 4.3, the interfacial pH increases at the potential where proton reduction and water reduction occur. However, the same interfacial pH is observed at the mass transport limited plateau irrespective of the cations present in the electrolytes.

4.3.2 Discussion

In the present work, we show a decreased diffusion limited current with increasing cation concentration in the electrolyte at pH 3. We assume the decreased diffusion limited current was due to the non-negligible migration current in electrolytes with low cation concentrations, given that the diffusion limited current is relatively stable and nearly the value as defined in the Levich equation in the presence of at least 50 mM perchlorate in the electrolyte. Although

previous work suggests a suppressed proton diffusion kinetics in presence of a high concentration of cations,³⁶ we believe that the decreased diffusion limited current observed here is mainly from the suppressed migration current under our working conditions, namely in electrolytes with cation concentration of ca. 100 mM.³⁷

In the presence of 80 mM KClO₄ or LiClO₄ as the supporting electrolyte, the improved onset potential for water reduction with increasing Li⁺ concentration indicates the essential role of cations for water reduction at pH 3 and the superior effect of Li⁺ cation in promoting water reduction on Pt electrode. Although previous work suggests an inhibition of HER by weakly hydrated cations on Pt, the unchanged water reduction current with increasing K⁺ concentration in pH 3 with 80 mM LiClO₄ as the supporting electrolyte indicates the inability of K⁺ in promoting water reduction at -0.57 V vs RHE. Further, interfacial pH measurements show a similar interfacial pH at Pt surface under diffusion limited conditions, which excludes the role of interfacial pH effect caused by cation hydrolysis near the electrode.^{35, 39} Consequently, neither a migration effect nor the local pH effect could explain the difference of 0.13 V in the onset of water reduction between Li⁺ and K⁺ containing electrolyte. Instead, our result suggests strongly hydrated cations (Li⁺) promote water dissociation more favorably compared to weakly hydrated cations (K⁺), under the conditions of the experiment.

The activity for CO₂RR products has been reported to increase in the order Cs⁺ > K⁺ > Na⁺ > Li⁺ on various electrodes in mild acidic media.⁴⁰⁻⁴¹ Although a different pathway has been reported for formic acid production, it has been proposed that weakly hydrated cations stabilize CO₂RR intermediates through local electrostatic interactions within the electrical double layer better than strongly hydrated cations.⁴⁰⁻⁴¹ Our results provide new insights into the competition between HER and CO₂RR on Pt based catalysts, a slower water reduction currents are expected with a weakly hydrated cation present in neutral or alkaline electrolyte. This could also add additional insights into the Faraday efficiency (FE) of 99% for HCOOH production at -0.1 V vs RHE on Pd catalysts in 2.8 M KHCO₃,⁴² where low HER activity are expected. Although further experiments are needed to prove this assumption, our results at least suggest that it is beneficial to employ weakly hydrated cations in mild acidic electrolyte

when the goal is to suppress HER on Pt-based catalysts.

4.4 Conclusions

We have investigated the cation concentration and identity effect in tuning the activity of HER on Pt electrode in mildly acidic electrolyte across a wide potential range. Our findings indicate that cations exhibit no discernible effect on proton reduction at low overpotentials. However, we identify a non-negligible migration current during proton reduction in electrolytes with low cation concentration, a current component which can be effectively suppressed by introducing adequate supporting electrolyte. Furthermore, our study delves into the essential role of cations, particularly Li^+ , in promoting water reduction on Pt electrodes. The promoting role of Li^+ is not related to migration effects or local pH effects, as K^+ does not promote water reduction, but still generates the same local pH. Our work hints at the potential benefits of utilizing weakly hydrated cations on Pt based catalysts if the goal is to suppress HER.

References

1. Sheng, W.; Gasteiger, H. A.; Shao-Horn, Y., Hydrogen Oxidation and Evolution Reaction Kinetics on Platinum: Acid vs Alkaline Electrolytes. *J. Electrochem. Soc.* **2010**, *157* (11), B1529.
2. Subbaraman, R.; Tripkovic, D.; Strmcnik, D.; Chang, K. C.; Uchimura, M.; Paulikas, A. P.; Stamenkovic, V.; Markovic, N. M., Enhancing hydrogen evolution activity in water splitting by tailoring Li(+)-Ni(OH)(2)-Pt interfaces. *Science* **2011**, *334* (6060), 1256-60.
3. Stamenkovic, V. R.; Strmcnik, D.; Lopes, P. P.; Markovic, N. M., Energy and fuels from electrochemical interfaces. *Nat Mater* **2016**, *16* (1), 57-69.
4. Strmcnik, D.; Lopes, P. P.; Genorio, B.; Stamenkovic, V. R.; Markovic, N. M., Design principles for hydrogen evolution reaction catalyst materials. *Nano Energy* **2016**, *29*, 29-36.
5. Ledezma-Yanez, I.; Wallace, W. D. Z.; Sebastián-Pascual, P.; Climent, V.; Feliu, J. M.; Koper, M. T. M., Interfacial water reorganization as a pH-dependent descriptor of the hydrogen evolution rate on platinum electrodes. *Nature Energy* **2017**, *2* (4).
6. Lamoureux, P. S.; Singh, A. R.; Chan, K., pH Effects on Hydrogen Evolution and Oxidation over Pt(111): Insights from First-Principles. *ACS Catal.* **2019**, *9* (7), 6194-6201.
7. Waagele, M. M.; Gunathunge, C. M.; Li, J.; Li, X., How cations affect the electric double layer and the rates and selectivity of electrocatalytic processes. *J. Chem. Phys.* **2019**, *151* (16), 160902.
8. McCrum, I. T.; Koper, M. T. M., The role of adsorbed hydroxide in hydrogen evolution reaction kinetics on modified platinum. *Nature Energy* **2020**, *5* (11), 891-899.
9. Goyal, A.; Koper, M. T. M., The Interrelated Effect of Cations and Electrolyte pH on the Hydrogen Evolution Reaction on Gold Electrodes in Alkaline Media. *Angew. Chem. Int. Ed. Engl.* **2021**, *60* (24), 13452-13462.
10. Goyal, A.; Koper, M. T. M., Understanding the role of mass transport in tuning the hydrogen evolution kinetics on gold in alkaline media. *J. Chem. Phys.* **2021**, *155* (13), 134705.
11. Huang, B.; Rao, R. R.; You, S.; Hpone Myint, K.; Song, Y.; Wang, Y.; Ding, W.; Giordano, L.; Zhang, Y.; Wang, T.; Muy, S.; Katayama, Y.; Grossman, J. C.; Willard, A. P.; Xu, K.; Jiang, Y.; Shao-Horn, Y., Cation- and pH-Dependent Hydrogen Evolution and Oxidation Reaction Kinetics. *JACS Au* **2021**, *1* (10), 1674-1687.
12. Monteiro, M. C. O.; Goyal, A.; Moerland, P.; Koper, M. T. M., Understanding Cation Trends for Hydrogen Evolution on Platinum and Gold Electrodes in Alkaline Media. *ACS Catal.* **2021**, *11* (23), 14328-14335.
13. Monteiro, M. C. O.; Dattila, F.; Lopez, N.; Koper, M. T. M., The Role of Cation Acidity on the Competition between Hydrogen Evolution and CO₂ Reduction on Gold Electrodes. *J. Am. Chem. Soc.* **2022**, *144* (4), 1589-1602.
14. Pentland, N.; Bockris, J. O. M.; Sheldon, E., Hydrogen Evolution Reaction on Copper, Gold, Molybdenum, Palladium, Rhodium, and Iron: Mechanism and Measurement Technique under High Purity Conditions. *J. Electrochem. Soc.* **1957**, *104* (3), 182.
15. Nørskov, J. K.; Bligaard, T.; Logadottir, A.; Kitchin, J. R.; Chen, J. G.; Pandelov, S.; Stimming, U., Trends in the Exchange Current for Hydrogen Evolution. *J. Electrochem. Soc.* **2005**, *152* (3), J23.
16. Rebollar, L.; Intikhab, S.; Oliveira, N. J.; Yan, Y.; Xu, B.; McCrum, I. T.; Snyder, J. D.; Tang, M. H., "Beyond Adsorption" Descriptors in Hydrogen Electrocatalysis. *ACS Catal.* **2020**, *10* (24), 14747-14762.

17. Rebollar, L.; Intikhab, S.; Snyder, J. D.; Tang, M. H., Kinetic Isotope Effects Quantify pH-Sensitive Water Dynamics at the Pt Electrode Interface. *J. Phys. Chem. Lett.* **2020**, *11* (6), 2308-2313.
18. Subbaraman, R.; Tripkovic, D.; Chang, K. C.; Strmcnik, D.; Paulikas, A. P.; Hirunsit, P.; Chan, M.; Greeley, J.; Stamenkovic, V.; Markovic, N. M., Trends in activity for the water electrolyser reactions on 3d M(Ni,Co,Fe,Mn) hydr(oxy)oxide catalysts. *Nat Mater* **2012**, *11* (6), 550-7.
19. Strmcnik, D.; Kodama, K.; van der Vliet, D.; Greeley, J.; Stamenkovic, V. R.; Markovic, N. M., The role of non-covalent interactions in electrocatalytic fuel-cell reactions on platinum. *Nat Chem* **2009**, *1* (6), 466-72.
20. Strmcnik, D.; Uchimura, M.; Wang, C.; Subbaraman, R.; Danilovic, N.; van der Vliet, D.; Paulikas, A. P.; Stamenkovic, V. R.; Markovic, N. M., Improving the hydrogen oxidation reaction rate by promotion of hydroxyl adsorption. *Nat Chem* **2013**, *5* (4), 300-6.
21. Liu, E.; Li, J.; Jiao, L.; Doan, H. T. T.; Liu, Z.; Zhao, Z.; Huang, Y.; Abraham, K. M.; Mukerjee, S.; Jia, Q., Unifying the Hydrogen Evolution and Oxidation Reactions Kinetics in Base by Identifying the Catalytic Roles of Hydroxyl-Water-Cation Adducts. *J. Am. Chem. Soc.* **2019**, *141* (7), 3232-3239.
22. Xue, S.; Garlyyev, B.; Watzele, S.; Liang, Y.; Fichtner, J.; Pohl, M. D.; Bandarenka, A. S., Influence of Alkali Metal Cations on the Hydrogen Evolution Reaction Activity of Pt, Ir, Au, and Ag Electrodes in Alkaline Electrolytes. *ChemElectroChem* **2018**, *5* (17), 2326-2329.
23. Kuhl, K. P.; Cave, E. R.; Abram, D. N.; Jaramillo, T. F., New insights into the electrochemical reduction of carbon dioxide on metallic copper surfaces. *Energy Environ. Sci.* **2012**, *5* (5), 7050-7059.
24. Cave, E. R.; Montoya, J. H.; Kuhl, K. P.; Abram, D. N.; Hatsukade, T.; Shi, C.; Hahn, C.; Nørskov, J. K.; Jaramillo, T. F., Electrochemical CO₂ reduction on Au surfaces: mechanistic aspects regarding the formation of major and minor products. *Phys. Chem. Chem. Phys.* **2017**, *19* (24), 15856-15863.
25. Gao, D.; Zhou, H.; Wang, J.; Miao, S.; Yang, F.; Wang, G.; Wang, J.; Bao, X., Size-dependent electrocatalytic reduction of CO₂ over Pd nanoparticles. *J. Am. Chem. Soc.* **2015**, *137* (13), 4288-91.
26. Ooka, H.; Figueiredo, M. C.; Koper, M. T. M., Competition between Hydrogen Evolution and Carbon Dioxide Reduction on Copper Electrodes in Mildly Acidic Media. *Langmuir* **2017**, *33* (37), 9307-9313.
27. Bondue, C. J.; Graf, M.; Goyal, A.; Koper, M. T. M., Suppression of Hydrogen Evolution in Acidic Electrolytes by Electrochemical CO₂ Reduction. *J. Am. Chem. Soc.* **2021**, *143* (1), 279-285.
28. Huang, J. E.; Li, F.; Ozden, A.; Sedighian Rasouli, A.; Garcia de Arquer, F. P.; Liu, S.; Zhang, S.; Luo, M.; Wang, X.; Lum, Y.; Xu, Y.; Bertens, K.; Miao, R. K.; Dinh, C. T.; Sinton, D.; Sargent, E. H., CO₂ electrolysis to multicarbon products in strong acid. *Science* **2021**, *372* (6546), 1074-1078.
29. Gu, J.; Liu, S.; Ni, W.; Ren, W.; Haussener, S.; Hu, X., Modulating electric field distribution by alkali cations for CO₂ electroreduction in strongly acidic medium. *Nat. Catal.* **2022**, *5* (4), 268-276.
30. Ma, Z.; Yang, Z.; Lai, W.; Wang, Q.; Qiao, Y.; Tao, H.; Lian, C.; Liu, M.; Ma, C.; Pan, A.; Huang, H., CO₂ electroreduction to multicarbon products in strongly acidic electrolyte via synergistically modulating the local microenvironment. *Nat. Commun.* **2022**, *13* (1), 7596.
31. Liu, X.; Monteiro, M. C. O.; Koper, M. T. M., Interfacial pH measurements during CO₂ reduction on gold using a rotating ring-disk electrode. *Phys. Chem. Chem. Phys.* **2023**, *25* (4), 2897-2906.
32. Chen, Q.-S.; Solla-Gullón, J.; Sun, S.-G.; Feliu, J. M., The potential of zero total charge of Pt nanoparticles and polycrystalline electrodes with different surface structure: The role of anion adsorption in fundamental electrocatalysis. *Electrochim. Acta* **2010**, *55* (27), 7982-7994.

33. Monteiro, M. C. O.; Liu, X.; Hagedoorn, B. J. L.; Snabilié, D. D.; Koper, M. T. M., Interfacial pH Measurements Using a Rotating Ring-Disc Electrode with a Voltammetric pH Sensor. *ChemElectroChem* **2021**, 9 (1).
34. van der Heijden, O.; Park, S.; Vos, R. E.; Eggebeen, J. J. J.; Koper, M. T. M., Tafel Slope Plot as a Tool to Analyze Electrocatalytic Reactions. *ACS Energy Lett.* **2024**, 9 (4), 1871-1879.
35. Singh, M. R.; Kwon, Y.; Lum, Y.; Ager, J. W., 3rd; Bell, A. T., Hydrolysis of Electrolyte Cations Enhances the Electrochemical Reduction of CO₂ over Ag and Cu. *J. Am. Chem. Soc.* **2016**, 138 (39), 13006-13012.
36. Li, X. Y.; Wang, T.; Cai, Y. C.; Meng, Z. D.; Nan, J. W.; Ye, J. Y.; Yi, J.; Zhan, D. P.; Tian, N.; Zhou, Z. Y.; Sun, S. G., Mechanism of Cations Suppressing Proton Diffusion Kinetics for Electrocatalysis. *Angew. Chem. Int. Ed. Engl.* **2023**, 62 (14), e202218669.
37. Amatore, C.; Fosset, B.; Bartelt, J.; Deakin, M. R.; Wightman, R. M., Electrochemical kinetics at microelectrodes: Part V. Migrational effects on steady or quasi-steady-state voltammograms. *J. Electroanal. Chem. Interfacial Electrochem.* **1988**, 256 (2), 255-268.
38. Bard, A. J.; Faulkner, L. R., *Electrochemical Methods: Fundamentals and Applications*. 2nd ed.; John Wiley & Sons 2001.
39. Ayemoba, O.; Cuesta, A., Spectroscopic Evidence of Size-Dependent Buffering of Interfacial pH by Cation Hydrolysis during CO₂ Electroreduction. *ACS Appl. Mater. Interfaces* **2017**, 9 (33), 27377-27382.
40. Monteiro, M. C.; Dattila, F.; Hagedoorn, B.; García-Muelas, R.; López, N.; Koper, M., Absence of CO₂ electroreduction on copper, gold and silver electrodes without metal cations in solution. *Nat. Catal.* **2021**, 4 (8), 654-662.
41. Ye, C.; Dattila, F.; Chen, X.; Lopez, N.; Koper, M. T. M., Influence of Cations on HCOOH and CO Formation during CO₂ Reduction on a Pd(ML)Pt(111) Electrode. *J. Am. Chem. Soc.* **2023**, 145 (36), 19601-19610.
42. Min, X.; Kanan, M. W., Pd-catalyzed electrohydrogenation of carbon dioxide to formate: high mass activity at low overpotential and identification of the deactivation pathway. *J. Am. Chem. Soc.* **2015**, 137 (14), 4701-8.